

# The most powerful quasar outflows as revealed by the CIV $\lambda 1549$ resonance line<sup>1</sup>

P. Marziani • M. A. Martínez Carballo •  
J. W. Sulentic • A. Del Olmo • G. M. Stirpe •  
D. Dultzin

**Abstract** While quasar outflows may be quasi-ubiquitous, there are significant differences on a source-by-source basis. These differences can be organized along the 4D Eigenvector 1 sequence: at least at low  $z$ , with only Population A sources radiating at relatively high Eddington ratio and showing prominent high-velocity outflows in CIV  $\lambda 1549$  line profiles. We discuss in this paper VLT-FORS observations of CIV  $\lambda 1549$  emission line profiles for a high-luminosity sample of Hamburg-ESO quasars and how they are affected by outflow motion as a function of quasar luminosity. Our high-luminosity sample has the notable advantage that the rest frame has been accurately determined from previous VLT-ISAAC observations of  $H\beta$  in the J, H, and K bands. This makes measures of inter-line velocity shifts accurate and free of systemic biases. As the redshift increases and the luminosity of the brightest quasars increases, powerful, high-velocity outflows become more frequent. We discuss the outflow contextualisation, following the 4DE1 formalism, as a tool for understanding the nature of the so-called weak lined quasars (WLQ)

discovered in recent years as a new, poorly understood class of quasars. We estimate the kinetic power associated with CIV  $\lambda 1549$  outflows and suggest that the host galaxies in the most luminous sources likely experience significant feedback.

**Keywords** galaxies: active; quasars: emission lines; quasars: general

## 1 Introduction

The optical and UV spectra of quasars show broad and narrow lines emitted by ionic species over a wide range of ionization potentials. A quasar spectrum is usually easily recognizable with the same emission lines almost always present and usually strong ( $W \sim 20 - 200 \text{ \AA}$ ) (with some exceptions §4.2) in all type-1 AGN. It is useful to distinguish between high- and low-ionization lines (hereafter HILs and LILs, respectively): CIV  $\lambda 1549$ , HeII  $\lambda 4686$ , HeII  $\lambda 1640$ , OVI  $\lambda 1035$  among the strongest HILs. Balmer ( $H\beta$ ,  $H\alpha$ ), optical FeII, MgII  $\lambda 2800$  and the CaII IR triplet are frequently observed LILs. We can also between high and low ionization narrow lines: [OIII]  $\lambda\lambda 4959, 5007$ , HeII  $\lambda 1640$ , HeII  $\lambda 4686$ , [NeIII] (HILs) and Balmer, OI  $\lambda 1304$ , SiII  $\lambda\lambda 6717, 6730$ , [NII]  $\lambda\lambda 6548, 6583$  (LILs). Apart from these commonalities, it is important to remark that quasars show widely differing line profiles, intensity ratios, and ionization levels (e.g., Marziani et al. 2015). This is made evident by a comparison between the prototypical Narrow Line Seyfert 1 (NLSy1) I Zw 1, and a broader line object like NGC 5548 (Sulentic et al. 2000). In this context it is especially important to stress that lines do not all show the same profiles. Internal emission line shifts involve both broad and narrow lines (Zamanov et al. 2002; Eracleous and Halpern 2003; Hu et al. 2008; Hewett and Wild 2010). Narrow LILs such

P. Marziani

INAF, Osservatorio Astronomico di Padova, Padova, Italia

M. A. Martínez Carballo

Instituto de Astrofísica de Andalucía (CSIC), Granada, Spain

J. W. Sulentic

Instituto de Astrofísica de Andalucía (CSIC), Granada, Spain

A. Del Olmo

Instituto de Astrofísica de Andalucía (CSIC), Granada, Spain

G. M. Stirpe

INAF, Osservatorio Astronomico di Bologna, Bologna, Italia

D. Dultzin

Instituto de Astronomía, UNAM, Mexico, D.F., Mexico

<sup>1</sup>Based in part on observations made with ESO Telescopes at the Paranal Observatory under programme 082.B- 0572(A), and on observations made with the Italian Telescopio Nazionale Galileo (TNG).

as narrow  $H\beta$  and  $[OII] \lambda 3727$  are the most suitable for estimating the quasar systemic redshift; however they are not easily observable at  $z > 1$  since they are shifted into the IR. Quasar systemic redshifts reported in literature are significantly more uncertain if  $z > 1$ . Systemic biases in the SDSS spectra as large as  $600 \text{ km s}^{-1}$  have been identified (Hewett and Wild 2010). They are of the same order of magnitude of internal emission line shifts between HILs and LILs in quasars (Gaskell 1982; Tytler and Fan 1992; Marziani et al. 1996; Corbin 1997).

There is general consensus that broadening of optical and UV emission lines is mostly associated with the Doppler effect reflecting emitting gas motions relative to the observer (scattering and gravitational redshift effects are not clearly assessed in quasar spectra e.g., Gaskell and Goosmann 2013). HIL blueshifts provide evidence of outflow (if the receding side of the outflow is hidden from view, as in an optically thick accretion disk with associated wind) but require rest frame knowledge and proper contextualisation for a correct analysis. A first contextualisation (e.g. radio quiet vs. radio loud; Sulentic et al. 1995; Corbin 1997) showed intriguing differences between RQ and RL quasars with large blueshifts observed only among RQ sources (§2). We discuss here our VLT-FORS CIV  $\lambda 1549$  spectra of high luminosity quasars (their location in the absolute magnitude vs. redshift plane is shown in Fig. 1) where a reliable rest frame could be estimated from narrow LILs, typically the narrow component of  $H\beta$  (§3). We report on the behaviour of the CIV  $\lambda 1549$  emission line profile as a function of luminosity, using the interpretative tools provided by the 4D eigenvector 1 approach (4DE1, §4). We derive inferences about the nature of weak-lined quasars (§4.2) and demonstrate that nuclear outflows traced by CIV  $\lambda 1549$  are expected to have a strong feedback effect on the host galaxy, especially for the most luminous Pop. A quasars (§5).

## 2 (4D)Eigenvector 1 quasar contextualization at low- $z$

The (4D) Eigenvector 1 quasar contextualization scheme at low- $z$  offers a powerful tool for interpretation of the CIV  $\lambda 1549$  emission line profile. Eigenvector 1 was originally defined from a Principal Component Analysis (PCA) of 87 PG quasars involving an anticorrelation between optical FeII intensity, half-maximum profile width of  $H\beta$  and peak intensity of  $[OIII] \lambda 5007$  (Boroson and Green 1992). E1 expanded to 4DE1 with the addition of X-ray photon index and CIV  $\lambda 1549$  profile shift measures (Sulentic et al. 2000, 2008, 2011).

4DE1 allows one to define a quasar main sequence in 4DE1 space (Sulentic et al. 2000; Marziani et al. 2001). The 4DE1 approach allows the definition of spectral types following source occupation in the optical plane  $FWHM(H\beta)$  vs  $R_{FeII}$  (Sulentic et al. 2002) and can be extended to include all four dimensions e.g. (Bachev et al. 2004). Along the sequence, it is possible to identify two populations: Population A with  $FWHM(H\beta) \leq 4000 \text{ km s}^{-1}$ , and a second Population B of sources with broader lines (see Sulentic et al. 2007, 2011, for the rationale behind two distinct quasar populations). Here we mention that, at low- $z$  ( $\lesssim 1.0$ ), Pop. A sources include narrow-line Seyfert 1s (NLSy1s) and strong Fe II<sub>opt</sub> emitters. Pop. B sources show weaker FeII emission and LIL emission broad profiles that are often redward asymmetric (Marziani et al. 2003a). In low- $z$  samples Pop. B sources are systematically more massive ( $M_{BH} \sim 10^9 M_{\odot}$ ) than Pop. A, and the wide majority of Fanaroff-Riley II powerful radio sources belongs to Pop. B (Zamfir et al. 2008). Pop. B sources could be therefore seen as more “evolved” AGN than Pop. A sources. Heuristic considerations and black hole and Eddington ratio estimates suggest that the principal driver of the quasar main sequence is Eddington ratio (e.g., Marziani et al. 2001, 2003b; Kuraszkiewicz et al. 2009). Population A and B are distinct in terms of Eddington ratio: the boundary value (for BH mass of  $10^8 M_{\odot}$ ) is estimated to be  $L/L_{Edd} \approx 0.2 \pm 0.1$  (Marziani et al. 2003b). It is interesting to note that this is the limit at which the transition from a geometrically thin to a geometrically thick disk is expected (Abramowicz et al. 1988; Frank et al. 2002, and references therein).

### 2.1 Interpretation of the CIV $\lambda 1549$ emission line profile along the 4DE1 sequence

The strongest emission lines can be empirically reproduced by 3 components with varying relative strength along the 4DE1 sequence (Marziani et al. 2010): (a) a blueshifted component (BLUE), strong in  $Ly\alpha$ , CIV  $\lambda 1549$ , HeII  $\lambda 1640$ ; (b) a “Broad Component” (BC), strong in all low ionization lines: Fe II<sub>opt</sub>, MgII  $\lambda 2800$ , H $\gamma$  Balmer lines; (c) a “Very Broad Component” (VBC  $FWHM \sim 10000 \text{ km s}^{-1}$ ; Peterson and Ferland 1986; Marziani and Sulentic 1993; Corbin 1997; Sulentic et al. 2000), redshifted; strong in  $Ly\alpha$ , CIV  $\lambda 1549$ , HeII  $\lambda 4686$ , Balmer lines but absent or at most weak in FeII.

Blueshifts have been associated with radial motion + obscuration since their discovery (Gaskell 1982). The blueshifted component is meant to isolate, in a heuristic way, the contribution of the radially-moving (most likely outflowing) gas. The approach is heuristic since,

in a multicomponent decomposition, we are isolating radial velocity components that may have no obvious counterpart in physical space. At the same time, inter-percentile velocity intensity ratios for the blue part of the profile are very different from the ones estimated over the core or of lines showing an almost symmetric profile. Since the emission line profiles originate in a spatially unresolved region, to ignore emission line shifts and asymmetries, and take an intensity ratio over the full profile can easily bring to misleading results. We can use Mark 478 as a representative example of spectral type A2, the most populated A spectral type; the same consideration apply to BLUE of the other A spectral type (Marziani et al. 2010). If the C IV  $\lambda 1549/\text{H}\beta$  ratio is computed over the full profile from the Mark 478 spectrum, it is  $\approx 19$ , for the unshifted BC component is  $\approx 1.4$ . Clear constraints on physical conditions emerge if the line components are considered individually. It is possible to measure fairly accurately the following intensity ratios for BLUE:  $\text{Ly}\alpha/\text{H}\beta$  ( $\gtrsim 30$ ), C IV  $\lambda 1549/\text{Ly}\alpha$  ( $\sim 0.5$ ), He II  $\lambda 1640/\text{C IV } \lambda 1549$  ( $\gtrsim 0.15$ ). Results of Cloudy 08.00 (Ferland et al. 1998, 2013) simulations as a function of density and ionization parameter  $U$  indicate that BLUE is consistent with high ionization ( $U \sim 10^{-1 \pm 0.5}$ ) and moderate density ( $n_{\text{H}} \sim 10^{9.5 \pm 0.5} \text{ cm}^{-2}$ ). The large  $\text{Ly}\alpha/\text{H}\beta \gtrsim 30$  is very different from the ones of the other components ( $\text{Ly}\alpha/\text{H}\beta \approx 5 - 10$ , Netzer et al. 1995). This latter value is difficult to explain for photoionization models. On the converse  $\text{Ly}\alpha/\text{H}\beta \gtrsim 30$  is expected under more standard physical conditions.

The decomposition involving BLUE is consistent with some models proposed in the past, such as those by Collin-Souffrin et al. (1986) and Elvis (2000). In the framework of these models, the blueshifted component is associated with radially outflowing clouds surrounding an accretion disk, or with a (non-rotating) wind driven by radiation pressure. There is fairly convincing evidence that strongest outflows are associated with the highest Eddington ratio values ( $L/L_{\text{Edd}}$ ; e.g., Boroson 2002; Marziani et al. 2003b; Baskin and Laor 2005; Richards 2012; Marziani et al. 2013b) where we indeed expect the strongest effect of radiation pressure.

Further interpretation of the heuristic decomposition of the broad profiles involves “stratification” of the emitting region: the broad component is associated with a lower ionization Broad Line Region (BLR), where line broadening is predominantly virial, and where Fe II, Ca II are emitted (Loli Martínez-Aldama et al. 2015, and references therein). The very broad component is associated with a high-ionization inner region, the Very Broad Line Region (VBLR) that emits no Fe II and shows lower continuum responsivity (Snedden and Gaskell 2007; Goad and Korista 2014). The

stratification is consistent with virial motions dominating the core of the Pop. B LILs. The LIL profiles often show asymmetries but the amplitude of the shifts is usually much less than the FWHM (Sulentic 1989; Marziani et al. 2003a; Zamfir et al. 2010). For reviews on the relation between emission line properties and accretion disk see Gaskell (2008) and Gaskell (2009).

## 2.2 Interpretation of the line profile: a narrow component for C IV $\lambda 1549$ ?

The long-slit spectra are far from resolving the broad line emitting region (size  $\sim 1 - 10$  pc). The half-slit width of 0.3 arcsec covers  $\approx \pm 2.5$  kpc from the nucleus. In addition to the BLR, a part of the (usually resolved) narrow line region (NLR) is included in the slit. The profiles of C IV  $\lambda 1549$  and  $\text{H}\beta$  are therefore the summation of contributions which may be separated (or overlapping) in radial velocity, but not necessarily spatially disjoint (or coincident). The interpretation of the line profile will follow a series of heuristic considerations which come from past analysis of large samples of high S/N spectra. As mentioned, we identified 4 main components: 1) the narrow component; 2) the broad component; 3) the very broad component; 4) a blueshifted component (Marziani et al. 2003b, 2010). The NC is partially resolved in nearby AGN. It is easily appreciable in the  $\text{H}\beta$  profile of Pop. B sources. Its presence has been debated for C IV  $\lambda 1549$ , several convincing arguments notwithstanding (Sulentic and Marziani 1999). Sulentic and Marziani (1999) ascribed the C IV  $\lambda 1549$  NC to the innermost, densest part of the NLR. Empirical isolation of the C IV  $\lambda 1549_{\text{NC}}$  is often ambiguous, as it merges smoothly with the underlying BC. While its contribution to the total C IV  $\lambda 1549$  flux is small, it can significantly affect line width measures. However, the very high luminosity of the HE sample may imply that the NC is contributing little to both BC flux and width (Netzer et al. 2004).

## 2.3 Modelling and measuring the broad C IV $\lambda 1549$ profile

Fig. 2 illustrates the C IV  $\lambda 1549$  line decomposition into a BC and a blueshifted component, for Pop. A, and into BC, VBC and blueshifted component for Pop. B (right panel). Radial velocities are measured for the peak intensity  $I_{\text{p}}$ , and for the centroids (black spots) at different fractional intensities. The same decomposition can be applied also to  $\text{H}\beta$ , although the blue shifted component is usually close to or below the noise level. Line centroids at fractional intensity are independent of multi-component decomposition, and will be considered for a quantitative statistical analysis in the following discussion.

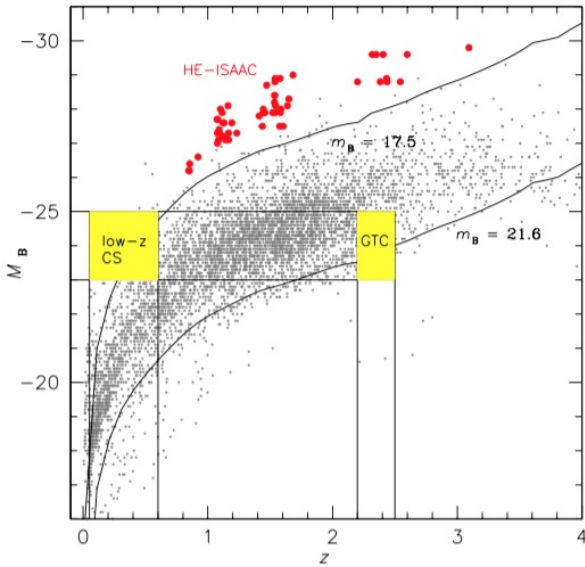


**Fig. 1** Absolute B magnitude vs  $z$  for the HE sample with ISAAC observations (red dots). A random subsample of the Véron-Cetty and Véron (2010) catalog is also plotted (grey dots). The absolute magnitude associated with two flux limits (17.5, appropriate for the HE survey) and (21.6, appropriate for the SDSS) are shown as function of redshift. Regions representing a low- $z$  control sample and a GTC sample of faint quasars at intermediate  $z$  (as described in Sulentic et al. 2014) are shown shaded in yellow.

### 3 Sample selection, observations and data analysis

Our sample was drawn from 52 quasars from the Hamburg-ESO survey (Wisotzki et al. 2000) observed with ISAAC in the  $H\beta$  spectral range to obtain reliable rest frames, in the redshift range  $0.9 \lesssim z \lesssim 3$  (most with  $z \lesssim 3$ ). The C IV  $\lambda 1549$  line was observable from ground ( $z \gtrsim 1.4$ ) for 32 sources, and C IV  $\lambda 1549$  was actually observed at TNG (equipped with DOLORES) and VLT (equipped with FORS2) for 28 quasars (hereafter the HE sample). The quasar HE sample includes 15 Pop. A and 17 Pop. B sources. A control sample (CS) for which  $H\beta$  and C IV  $\lambda 1549$  observations are available at low  $z$  and low luminosity was extracted from 130 HST/FOS C IV  $\lambda 1549$  observations (Sulentic et al. 2007). Fig. 1 illustrates the placement of the CS and of the HE sample in the absolute magnitude vs. redshift plane. In this paper we will use all of the 130 FOS observations, which means the addition of a minority of sources more luminous than  $M_B \approx -25$ . An additional sample of GTC observations of faint quasars at high- $z$  has been also used, to help distinguish redshift from  $L$  effects.

Previous observations of  $H\beta$  for the HE sample were discussed in a series of papers (Sulentic et al. 2004,

2006b; Marziani et al. 2009). Data analysis has been carried out with multicomponent maximum-likelihood fits in both the UV and optical rest-frame range. The IRAF task SPECFIT (Kriss 1994) allows for the inclusion of most-frequently observed components in the spectra of extragalactic sources. Specific to the analysis of C IV  $\lambda 1549$  and  $H\beta$  in quasars, we considered a local power-law, Fe II emission represented by a scaled and broadened template. Narrow lines were fit with Gaussians, while broad C IV  $\lambda 1549$  and  $H\beta$  were fit using Lorentzian and/or Gaussians, depending on Population as described below.

## 4 Results

Fig. 3 provides examples of Pop. A and Pop. B sources in the HE sample, with the  $H\beta$  and C IV  $\lambda 1549$  spectral ranges shown side-by-side. The result of the SPECFIT analysis carried out for these objects is shown in Fig. 4. A most remarkable finding is that the C IV  $\lambda 1549$  profiles show significant blueshifts with respect to the rest frame (dot-dashed line) for both Pop. A and B. The amplitude of the blueshifts are however larger for Pop. A than for Pop. B. A detailed analysis of the full dataset will be presented elsewhere. Here we focus on results concerning the relation between blueshift and quasar luminosity.

### 4.1 Luminosity and radio-loudness effects on quasars blueshifts

The significance of these results can be appreciated by comparing the distribution of C IV  $\lambda 1549$  line shifts (centroid at half maximum,  $c(\frac{1}{2})$ ) in four luminosity bins (Fig. 5). The two panels for  $\log L \geq 47$  show the distribution for the HE sample, while the distributions at lower luminosity are drawn from the control sample. The left panel isolates Pop. A (shaded blue) while the right one RL sources (shaded red). Pop. A sources are associated with the largest shifts, while RL sources dominate the redshifted part of the distribution at low  $z$ . It is not the case that RL sources do not show any blue shift; however the blueshift amplitudes rarely exceed  $1000 \text{ km s}^{-1}$ , and the luminosity dependence is shallower than for RQ (Richards et al. 2011). We can consider that the effect of radio loudness on  $H\beta$  is not remarkable, if the comparison is restricted to Pop. B sources, as appropriate since there are very few Pop. A RQ. The redward asymmetry seen in Pop. B RL is seen in Pop. B RQ as well (Marziani et al. 2003b; Zamfir et al. 2010). It does not seem that the redward asymmetry is a phenomenon exclusive to RL sources

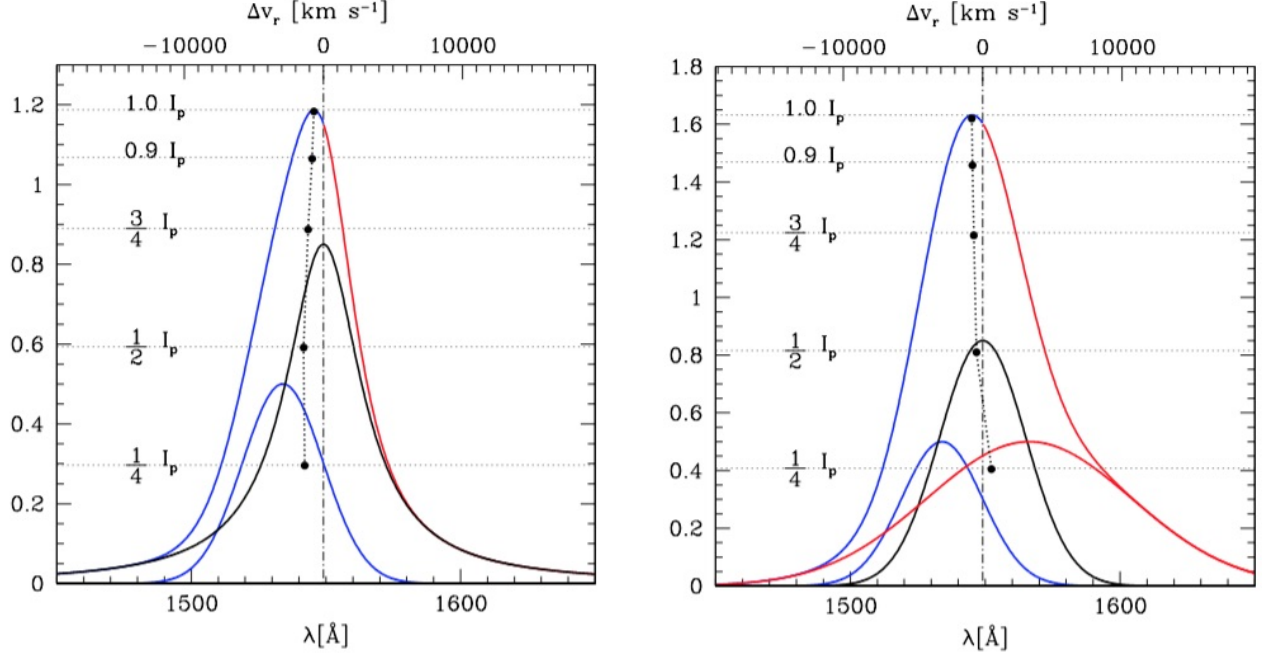


**Fig. 2** Mock CIV  $\lambda 1549$  profile illustrating the line decomposition into a BC and a blueshifted component for Pop. A (left), and into a BC, VBC and blue shifted component for Pop. B (right). Radial velocities are measured for the peak intensity  $I_p$ , and the centroids (black spots) at different fractional intensities on the *full* profile, to obtain a quantitative parameterisation that is independent of the decomposition of the profile.

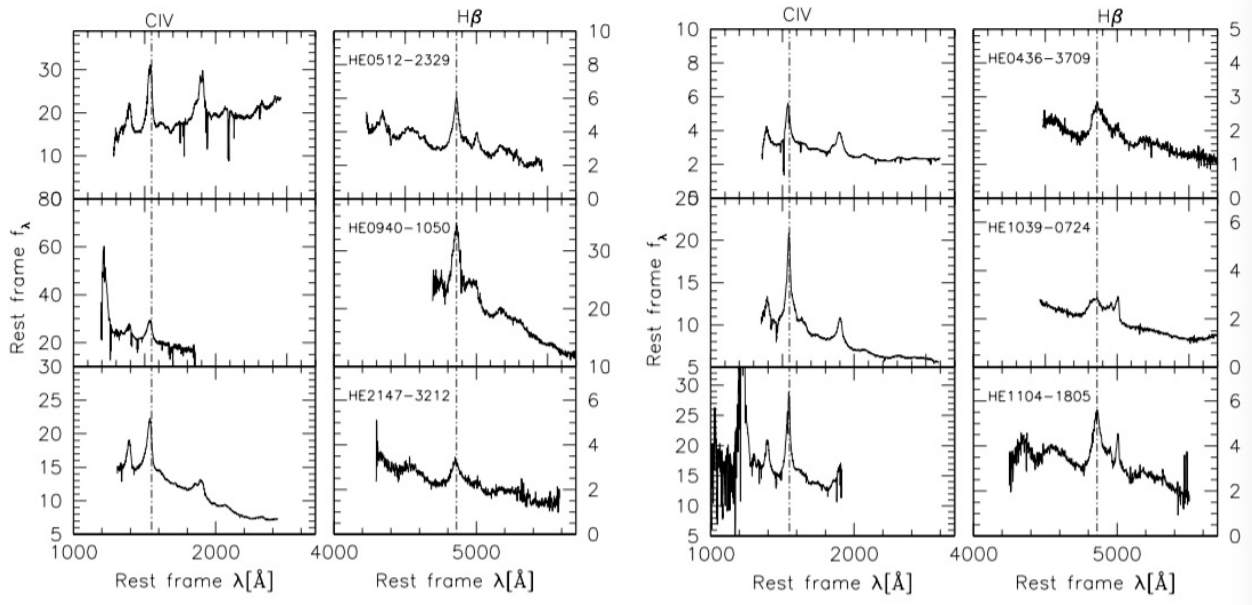


**Fig. 3** Spectra of sources in the HE sample, in the CIV  $\lambda 1549$  and H $\beta$  spectral range, for Pop. A (left) and Pop. B (right). Abscissæ are rest frame wavelength in Å, ordinates are specific flux in units of  $10^{-15}$  ergs s<sup>-1</sup> cm<sup>-2</sup> Å<sup>-1</sup>.



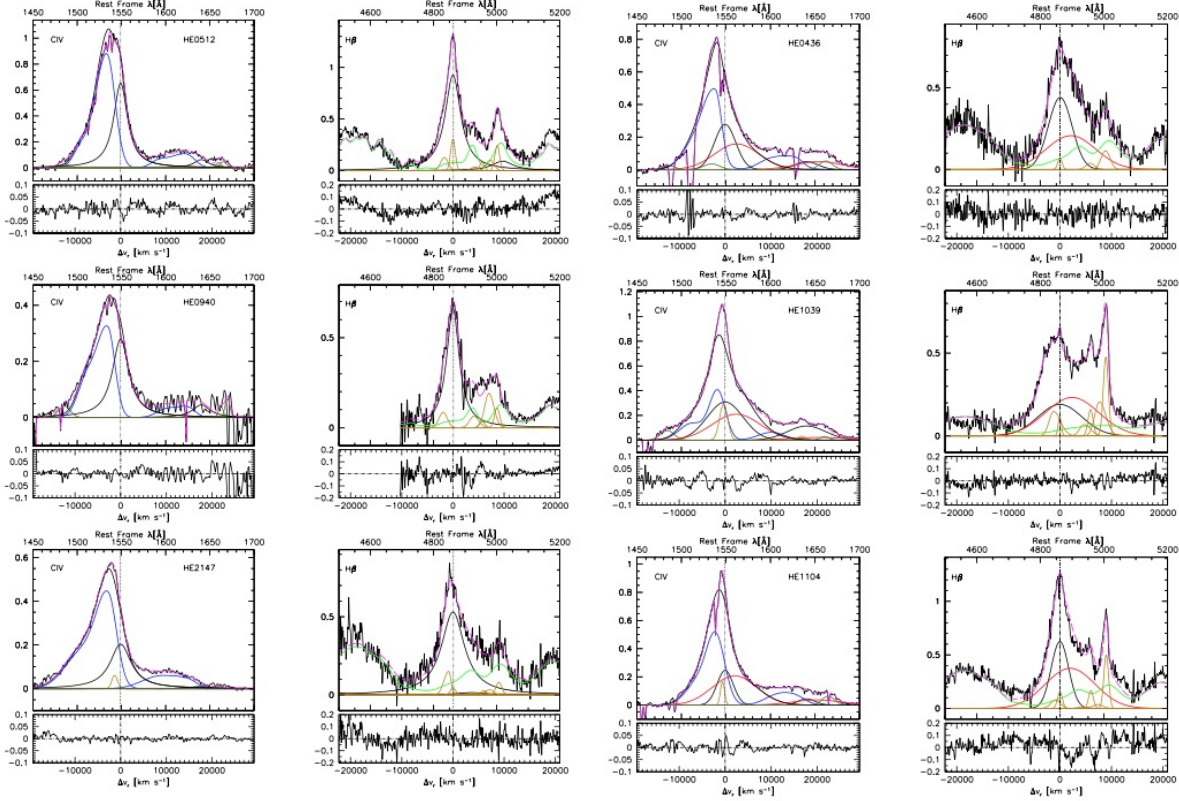


**Fig. 4** Spectra of sources in the HE sample, in the CIV  $\lambda 1549$  and  $H\beta$  spectral range, for Pop. A (left) and Pop. B (right), after continuum subtraction. Horizontal scale is rest frame wavelength in  $\text{\AA}$  or radial velocity shift from CIV  $\lambda 1549$  rest wavelength (left) or  $H\beta$  (right) marked by dot dashed lines; vertical scale is intensity normalized to specific flux at continuum adjacent the two emission lines. The panels show the emission line components used in the fit: FeII emission (green), broad and very broad component (red, for Pop. B only), and BLUE (blue). Lower panels show residuals observed - SPECIFIT model.

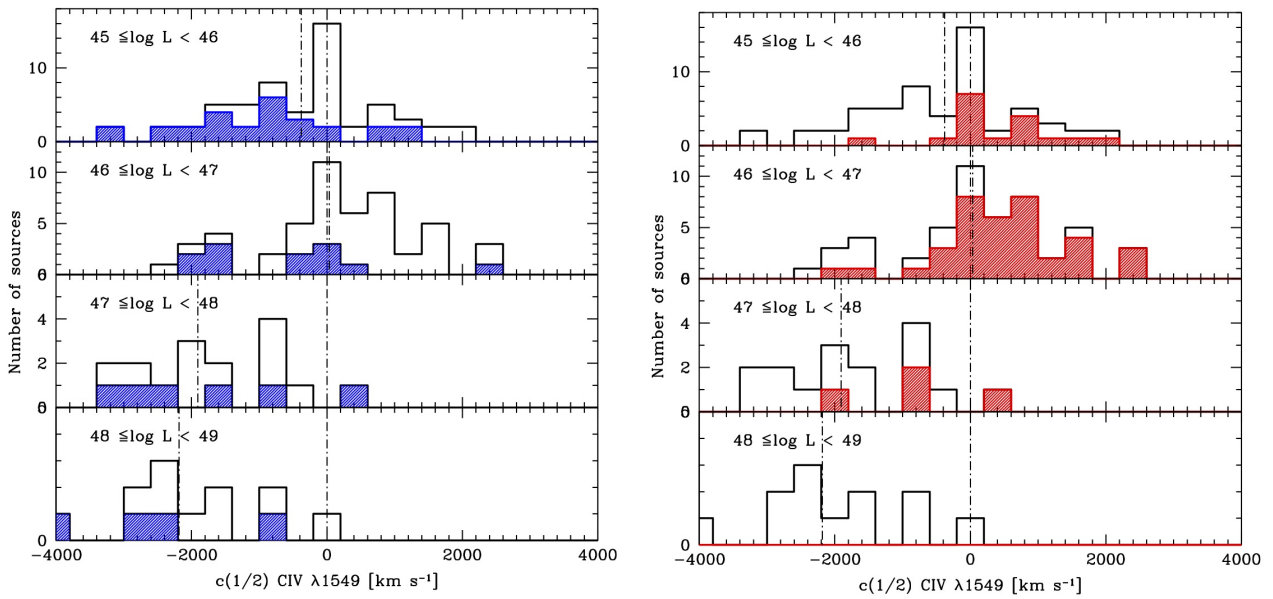


**Fig. 5** Distribution of CIV  $\lambda 1549$  centroids at half maximum, in  $\text{km s}^{-1}$ , in four quasar luminosity ranges, for the CS and HE samples. Left: the distribution of Population A sources is shaded blue; right: RL distribution is shaded red.

(Punsly 2010; Punsly and Zhang 2011), as it is most prominent right in the HE sample Pop. B sources that are mostly RQ. Therefore a proper contextualization may follow the scheme of Fig. 6: while for LILs it is sufficient to separate Pop. A and B to avoid mixup of sources in different dynamical conditions, for HIL analysis it is necessary to distinguish between Pop. B RQ and RL. The color coding in Fig. 6 reflects the average Civ  $\lambda 1549$  centroid shifts at half maximum in the sample of Sulentic et al. (2007):  $c(\frac{1}{2}) \approx -900, -250, +70 \text{ km s}^{-1}$  for Pop. A RQ, Pop. B RQ, and Pop. B RL respectively. The weakness of the blueshifts in RL sources makes the redward asymmetry in Civ  $\lambda 1549$  more easily detectable, so that the RL Civ  $\lambda 1549$  profile either look more symmetric or even redshifted (Fig. 5), while the Civ  $\lambda 1549$  profiles of RQ Pop. B sources are more affected by blue shifted emission, resulting in a smaller net blueshift on average.

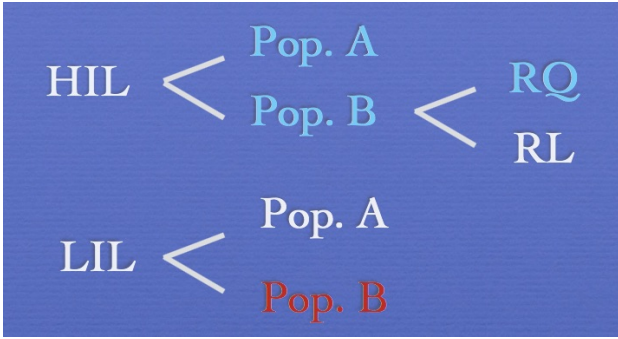


**Fig. 6** Contextualization scheme for HILs and LILs. Separation of RL and RQ is needed for HILs only in Pop. B. The color coding indicates a predominant blueshift (pale blue), no significant shift (white), and a predominant redshift (red).

Fig. 5 indicates that blueshifts are more frequent at high luminosity, and that the shift amplitude tends to increase as a function of luminosity. This is also shown by Fig. 7: the blueshift amplitude at the line base depends strongly on continuum luminosity, although it is probably misleading to interpret the diagram in terms of a correlation: at each luminosity there is a large range in shifts. In Fig. 7 we considered twice the  $c(\frac{1}{4})$  as a proxy (as a matter of fact, an underestimate) of the terminal velocity  $v_t$  associated with a wind. In the case of a radiation driven wind,  $v_t$  can be written as:

$$v_t \sim v_K \sqrt{\mathcal{M} \frac{L}{L_{\text{Edd}}}} \sim \sqrt{\frac{GM}{L^{\frac{1}{2}}}} \sqrt{\mathcal{M} \frac{L}{M}} \quad (1)$$

where we have assumed that the Keplerian velocity can be written as  $v_K^2 = GM/R$ , and that the radius scales with the square root of the luminosity, as found from

reverberation mapped sources (Bentz et al. 2006, 2009). If the force multiplier  $\mathcal{M}$  does not depend on  $L$ , then  $v_t \propto L^{\frac{1}{4}}$ . In other words, in the case of a radiation driven wind, under the simplest assumptions, we expect a pure luminosity dependence (Laor and Brandt 2002, c.f. Marziani et al. 2013b). The line drawn in Fig. 7 for an arbitrary normalisation shows that a trend  $|v_t| \sim 2c(\frac{1}{4}) \propto L^{\frac{1}{4}}$  is consistent with the systematic increase in Pop. A blueshifts (a different normalisation would account for Pop. B sources as well).

The dynamical relevance of the Civ  $\lambda 1549$  shift i.e., the shift amplitude normalized by the line half-width at half-maximum of  $H\beta$  (Marziani et al. 2013a), is  $|\Delta v(\frac{1}{2})|/\text{WHM}(H\beta) \gtrsim 1$  in the most extreme quasars. As is possible to appreciate from Fig. 4, the Civ  $\lambda 1549$  line is almost blueshifted with respect to the rest frame of the quasar. However, we do not see a strong dependence on line luminosity: the largest normalised shifts are observed in the control sample, at moderate  $L$  ( $\log L \sim 44$ ; right panel of Fig. 7).

#### 4.2 Extreme outflows in extreme quasars: weak lined quasars

Weak Lined Quasars (WLQs) have been a surprising discovery, since they are radio quiet quasars with usually low equivalent width of Civ  $\lambda 1549$  ( $\leq 10\text{\AA}$ ) and  $\text{Ly}\alpha$  ( $\leq 16\text{\AA}$ , Diamond-Stanic et al. 2009; Shemmer et al. 2010). The insight gained by the contextualization of low redshift quasars Civ  $\lambda 1549$  profiles allows to frame them relatively easily. Pop. A sources, in the 4DE1 context, show lower  $W(\text{Civ } \lambda 1549)$  (Bachev et al. 2004; Sulentic et al. 2007), and among them we also found the most extreme blueshifts. We can consider at first the behaviour of the Civ  $\lambda 1549$  shifts versus equivalent width (Fig 8). Of the five sources (3 in the CS and 2 HE) all low equivalent width sources show large Civ  $\lambda 1549$  blueshifts ( $\lesssim -1000 \text{ km s}^{-1}$ ). The same results holds for the WLQs recently observed by Plotkin et al. (2015), with simultaneous  $H\beta$  and Civ  $\lambda 1549$  coverage. Looking at the optical plane of the 4DE1 space (Fig. 9), we see that all 10 WLQs (CS, HE, and Plotkin et al. 2015) are Pop. A sources, and most of them in the domain of extreme Population A with  $R_{\text{FeII}} \gtrsim 1$ . Apart from the Civ  $\lambda 1549$  line, other features in the UV spectra are consistent with extreme A quasars revealed at both high and low luminosity, radiating at high Eddington ratio (Dultzin et al. 2011; Negrete et al. 2012; Marziani and Sulentic 2014). We conclude that WLQs should be considered extreme Pop. A sources, probably among the quasars accreting at the highest rate. This view is supported by the optical and soft-X analysis of Luo et al. (2015) who found X-ray properties consistent

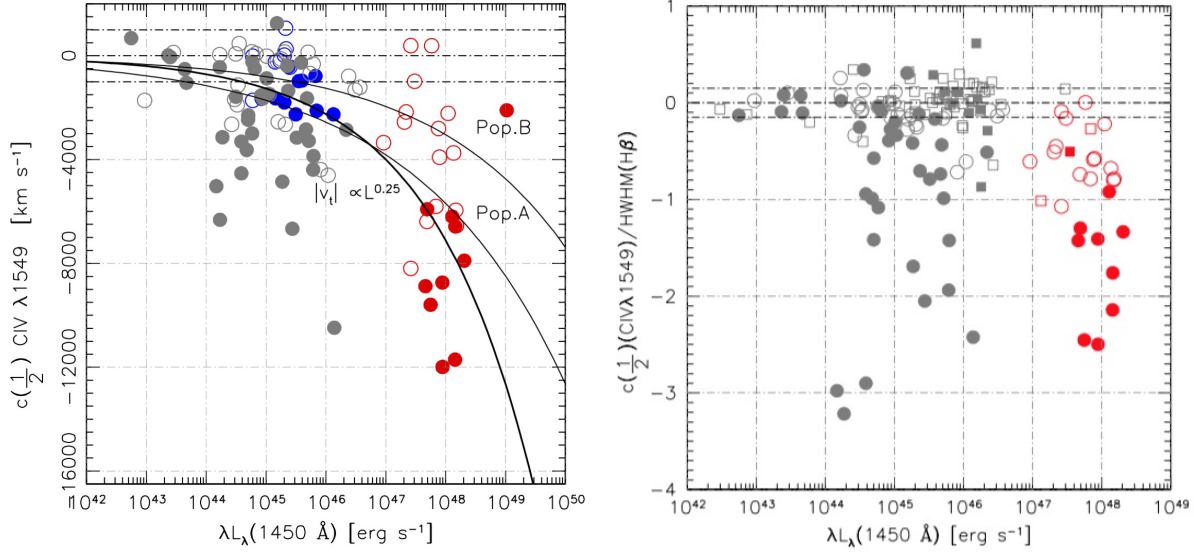


**Fig. 7** Behaviour of the CIV  $\lambda 1549$  emission line shifts as a function of continuum luminosity. Left:  $2 c(\frac{\lambda}{2})$  vs continuum luminosity at  $1450 \text{ \AA}$ . The thick black line shows the simple radiation-driven wind prediction,  $2 |c(\frac{\lambda}{2})| \propto L^{\frac{1}{4}}$ , the thin lines the best fit for Pop. A and B sources. Filled circles are Pop. A, open circles Pop. B. Data points refer to the CS (grey), to the HE sample (red) and to the faint high- $z$  sample of Sulentic et al. (2014, , blue). Right: dynamical relevance parameter  $c(\frac{\lambda}{2}) / \text{HWHM}(\text{H}\beta)$  vs luminosity. Filled symbols are Pop. A; open Pop. B; circles RQ, squares RL. The dot-dashed lines limit the region where lines could be considered unshifted.

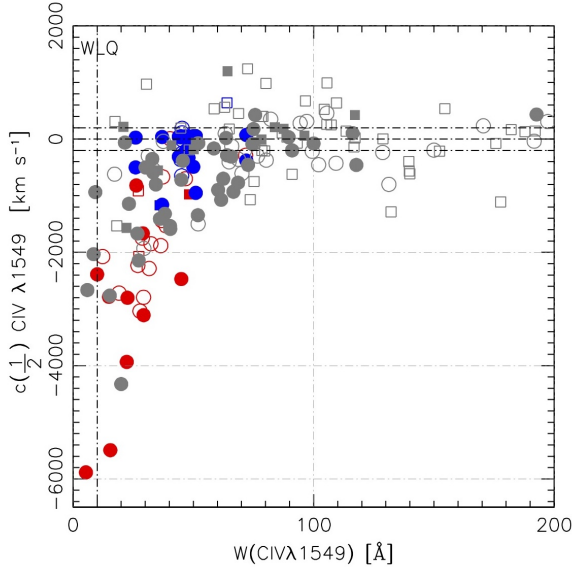


**Fig. 8** CIV  $\lambda 1549$  shift in  $\text{km s}^{-1}$  vs rest frame  $W(\text{CIV } \lambda 1549)$  in  $\text{\AA}$ . Filled symbols are Pop. A; open Pop. B; circles RQ, squares RL. The vertical dot-dashed line limits the region of WLQs. Data points refer to the CS (grey), to the HE sample (red) and to the faint high- $z$  sample of Sulentic et al. (2014, , blue).

with X-ray shielding by a thick structure possibly the “slim” disk expected at high accretion rate (§2).

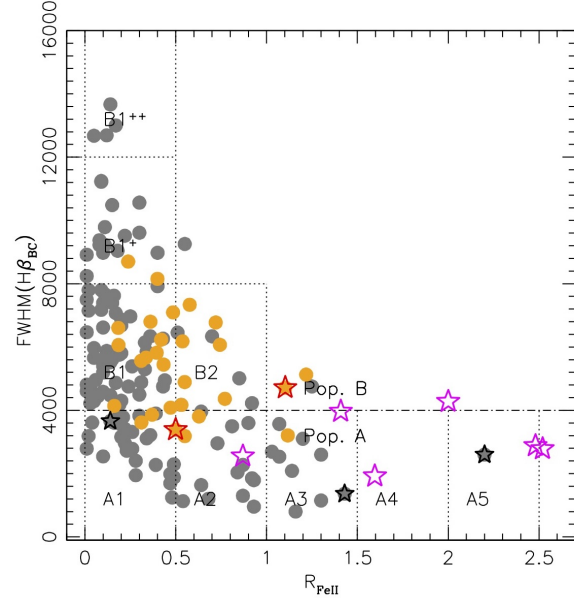


**Fig. 9** The optical 4DE1 plane,  $\text{FWHM}(\text{H}\beta)$  vs.  $R_{\text{FeII}}$ . Orange: HE data, grey: data from Sulentic et al. (2007). The stars identify the WLQs in the Sulentic et al. (2007) sample (black), in the HE sample (red), and in the Plotkin et al. (2015) paper (magenta).



## 5 Discussion: what do the most powerful outflows mean for galaxy evolution?

The most powerful outflows are believed to produce significant feedback effects on the host galaxies (Reeves et al. 2009; Rupke and Veilleux 2011; Fabian 2012). The observational evidence of the active nucleus feedback is still debated, and rest upon the discovery of ultra-fast outflows (UFOs, Tombesi et al. 2010), whose X-ray features are still passible of alternative interpretation. Large Balnicity index BAL QSOs are a minority of quasars (Vestergaard 2003; Sulentic et al. 2006a; Trump et al. 2006). On the converse, quasars outflows are observed in most radio quiet quasars (90% of all quasars). An order of magnitude estimate of the kinetic power associated with the CIV  $\lambda 1549$  emitting outflows is possible under several assumptions that make the estimate uncertain but not unrealistic (Fabian 2012; Cano-Díaz et al. 2012; King and Pounds 2015). We start considering the fraction of the flux in the CIV  $\lambda 1549$  blue component that is above the expected projected escape velocity at  $r \sim 1000 R_g$ . The assumed  $r$  is relatively large in the BLR context and will yield a lower limit to the kinetic power.

The CIV  $\lambda 1549$  line luminosity associated with the outflow above escape velocity is given by

$$L(\text{CIV}) = \int_V j_{\text{CIV}} f_f dV,$$

(where  $f_f$  is the filling factor, and  $j_{\text{CIV}}$  is the line emissivity per unit volume) which can be written as:

$$j_{\text{CIV}} = h\nu q_{\text{lu}} n_e n_l,$$

for a collisionally excited line, where  $n_e$  is the electron density and  $n_l$  the number density of  $\text{C}^{3+}$  ions at the transition lower level. The collisional excitation rate  $q_{\text{lu}}$  (Osterbrock and Ferland 2006) is given by

$$q_{\text{lu}} = \frac{\beta}{\sqrt{T}} \frac{\Upsilon_{\text{lu}}}{g_l} \exp\left(-\frac{\epsilon_{\text{lu}}}{kT}\right)$$

where  $g_l$  is the statistical weight of the lower level,  $\Upsilon_{\text{lu}}$  the effective collision strength,  $T_e$  the electron temperature,  $\epsilon_{\text{lu}}$  the energy level difference, and  $\beta$  a constant. The CIV  $\lambda 1549$  line luminosity can be connected to the mass of outflowing ionized gas  $M_{\text{out}}^{\text{ion}}$ , by considering that the  $M_{\text{out}}^{\text{ion}}$  can be written as, under the assumption of constant density:

$$M_{\text{out}}^{\text{ion}} = 9.5 \cdot 10^2 L_{45}(\text{CIV}) \left(\frac{Z}{5Z_{\odot}}\right)^{-1} n_9^{-1} M_{\odot}$$

where the metallicity  $Z \approx 5Z_{\odot}$  is appropriate for luminous high  $z$  quasars (Hamann and Ferland 1993; Nagao et al. 2010), and  $n_9$  is the density in units of  $10^9 \text{ cm}^{-3}$ . The mass outflow rate at a distance  $r$  (1 pc) can be written, if the flow is confined to a solid angle of  $\Omega$ , as:

$$\dot{M}_{\text{out}}^{\text{ion}} = \rho \Omega r^2 v = \frac{M_{\text{out}}^{\text{ion}}}{V} \Omega r^2 v \approx 15 L_{45} v_{5000} r_1^{-1} M_{\odot} \text{ yr}^{-1}$$

The outflow kinetic power, with outflow  $v$  in units of  $5000 \text{ km s}^{-1}$ , is:

$$\dot{\epsilon} = \frac{1}{2} \dot{M}_{\text{out}}^{\text{ion}} v^2 \approx 1.2 \cdot 10^{44} L_{45} v_{5000}^3 r_1^{-1} \text{ erg s}^{-1}.$$

The total energy expelled over a duty cycle of  $10^8$  yr is

$$\int \dot{\epsilon} dt \sim 4 \cdot 10^{59} L_{45} v_{5000}^3 r_1^{-1} \tau_8 \text{ erg}.$$

This value can be compared to the binding energy of the gas in a massive bulge/spheroid of mass  $M_{\text{sph}}$ :

$$U = \frac{3GM_{\text{sph}}^2 f_g}{5R_e} \sim 2 \cdot 10^{59} M_{\text{sph},11}^2 f_{g,0.1} R_{e,2.5\text{kpc}}^{-1} \text{ erg},$$

where  $R_e$  is the effective radius in units of 2.5 kpc, and  $f_{g,0.1}$  is the gas mass ratio in units of 0.1. Fig. 10 shows the distribution of the blue shifted component luminosity above the escape velocity at  $1000 R_g$  (left panel). The distribution of the corresponding kinetic powers is shown in the right panel of Fig. 10, for Pop. A and B HE sources separately. The luminosity values are enormous, comparable to the bolometric luminosity of bright quasars in the local Universe, and the kinetic energy deposited over a quasar life cycle is comparable to the binding energy of a massive spheroid. We have assumed an escape radius of  $1000 R_g$ , and density  $n_9 = 1$ . Both parameters could likely have lower values, making our estimates lower limits to the  $M_{\text{out}}^{\text{ion}}$  and hence to the kinetic power. Consistent results come from an analogous analysis of the [OIII]  $\lambda\lambda 4959, 5007$  blue shifted emission. It is possible that we are, at least in part, considering the same outflows. However, if the [OIII]  $\lambda\lambda 4959, 5007$  outflows can also be due to extranuclear star formation, this is very unlikely for the CIV  $\lambda 1549$  broad line, that can be safely associated with processes occurring in the active nucleus. We also note that the WLQs do contribute significant kinetic power the low line equivalent widths notwithstanding, also because their line blueshifts are among the largest ever observed.

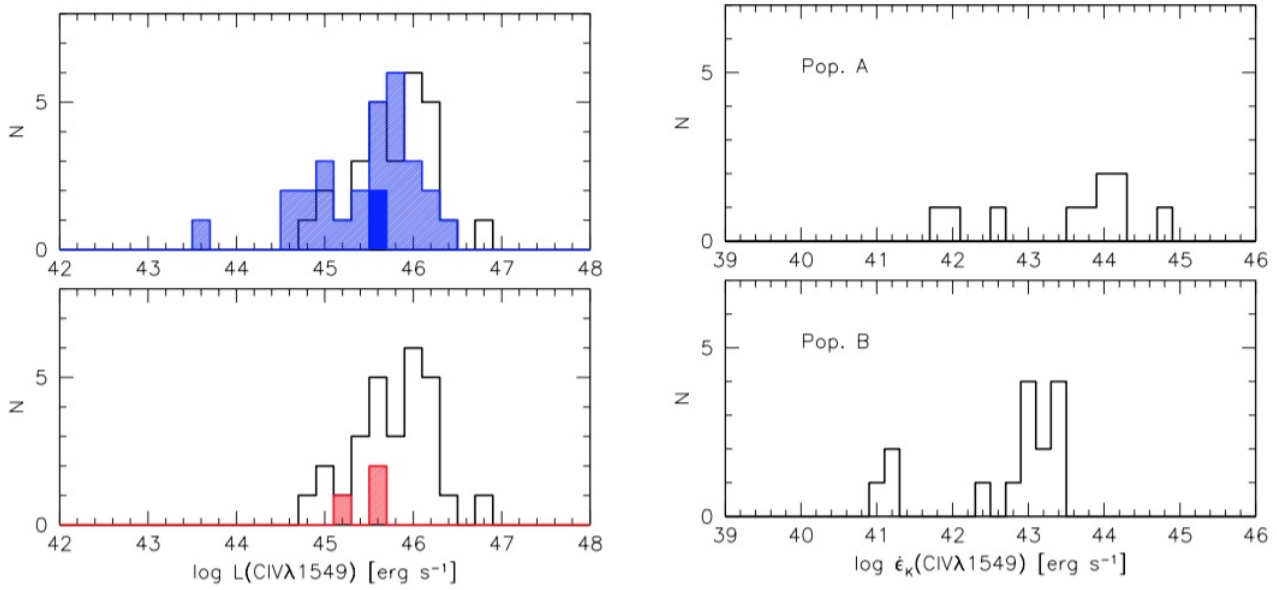


**Fig. 10** Left: Distribution of CIV  $\lambda 1549$  emission line luminosity, in ergs s<sup>-1</sup>. Top panel: shaded blue is the fraction above projected escape velocity. Dark blue identifies WLQs. Bottom panel: same as top, with the identification of RL sources. Right: distribution of kinetic power for Pop. A (top) and Pop. B (bottom), in units of ergs s<sup>-1</sup>.

## 6 Conclusion

4DE1 provides an interpretation framework at low as well as at extreme luminosity. The CIV  $\lambda 1549$  analysis reveals blueshifted emission associated with quasars outflows in RQ quasars, with high amplitude shifts being apparently more frequent at high  $L$ . Contextualization of HIL requires not only a distinction between Pop. A and B, but also that RL and RQ sources are kept separate, with RL sources showing blueshifts of systematically lower amplitude, no shifts or even redward asymmetric CIV  $\lambda 1549$  profiles. “Unexpected” luminosity effects are not seen (§4.1): larger CIV  $\lambda 1549$  shifts at high  $L$  are expected for a simple radiation-driven wind. Otherwise, the outflow phenomenology is self-similar over a wide range of  $L$ : Fig. 7 shows that large blueshifts ( $\gtrsim 1000$  km s<sup>-1</sup>) are possible over at least a 4.5 dex in luminosity, and that the CIV  $\lambda 1549$  shift “dynamical relevance” is distributed over the same range at moderate and high  $L$ . The most extreme cases of blueshifts include the WLQs that, in the 4DE1 context, are revealed to be predominantly extreme accretions (i.e., WLQs belong to the xA class of Marziani and Sultentic 2014). The CIV  $\lambda 1549$  blueshift-dominated profile in the most luminous sources supports the idea that a nuclear outflow may be at the origin of galactic-scale feedback effects.

We thank the referee, Martin Gaskell, for suggestions that improved the presentation of the paper, and

a second anonymous reviewer for suggesting an important reference. AdO and JS acknowledge the support by the Junta de Andalucía through project TIC114, and the Spanish Ministry of Economy and Competitiveness (MINECO) through project AYA2013-42227-P. PM acknowledges the hospitality of the Instituto de Astrofísica de Andalucía (IAA-CSIC) where part of this work was done. The TNG is operated on the island of La Palma by the Fundación Galileo Galilei of the INAF (Istituto Nazionale di Astrofisica) at the Spanish Observatorio del Roque de los Muchachos of the Instituto de Astrofísica de Canarias.

## References

- Abramowicz, M.A., Czerny, B., Lasota, J.P., Szuszkiewicz, E.: *Astrophys. J.* **332**, 646 (1988). doi:10.1086/166683
- Bachev, R., Marziani, P., Sulentic, J.W., Zamanov, R., Calvani, M., Dultzin-Hacyan, D.: *ApJ* **617**, 171 (2004). arXiv:astro-ph/0408334. doi:10.1086/425210
- Baskin, A., Laor, A.: *MNRAS* **356**, 1029 (2005). arXiv:astro-ph/0409196. doi:10.1111/j.1365-2966.2004.08525.x
- Bentz, M.C., Peterson, B.M., Pogge, R.W., Vestergaard, M., Onken, C.A.: *ApJ* **644**, 133 (2006). arXiv:astro-ph/0602412. doi:10.1086/503537
- Bentz, M.C., Peterson, B.M., Pogge, R.W., Vestergaard, M.: *ApJL* **694**, 166 (2009). 0812.2284. doi:10.1088/0004-637X/694/2/L166
- Boroson, T.A.: *Astrophys. J.* **565**, 78 (2002). arXiv:astro-ph/0109317. doi:10.1086/324486
- Boroson, T.A., Green, R.F.: *ApJS* **80**, 109 (1992). doi:10.1086/191661
- Cano-Díaz, M., Maiolino, R., Marconi, A., Netzer, H., Shemmer, O., Cresci, G.: *Astron. Astrophys.* **537**, 8 (2012). 1112.3071. doi:10.1051/0004-6361/201118358
- Collin-Souffrin, S., Joly, M., Pequignot, D., Dumont, S.: *Astron. Astrophys.* **166**, 27 (1986)
- Corbin, M.R.: *ApJS* **113**, 245 (1997). doi:10.1086/313058
- Diamond-Stanic, A.M., Fan, X., Brandt, W.N., Shemmer, O., Strauss, M.A., Anderson, S.F., Carilli, C.L., Gibson, R.R., Jiang, L., Kim, J.S., Richards, G.T., Schmidt, G.D., Schneider, D.P., Shen, Y., Smith, P.S., Vestergaard, M., Young, J.E.: *Astrophys. J.* **699**, 782 (2009). 0904.2181. doi:10.1088/0004-637X/699/1/782
- Dultzin, D., Martínez, M.L., Marziani, P., Sulentic, J.W., Negrete, A.: In: et al. (Eds.), L.F. (ed.) *Proceedings of the conference "Narrow-Line Seyfert 1 Galaxies and their place in the Universe"*. April 4-6, 2011. Milano, Italy. *Proceedings of Science*, (2011)
- Elvis, M.: *Astrophys. J.* **545**, 63 (2000). arXiv:astro-ph/0008064. doi:10.1086/317778
- Eracleous, M., Halpern, J.P.: *ApJ* **599**, 886 (2003). arXiv:astro-ph/0309149. doi:10.1086/379540
- Fabian, A.C.: *Annu. Rev. Astron. Astrophys.* **50**, 455 (2012). 1204.4114. doi:10.1146/annurev-astro-081811-125-521
- Ferland, G.J., Korista, K.T., Verner, D.A., Ferguson, J.W., Kingdon, J.B., Verner, E.M.: *PASP* **110**, 761 (1998). doi:10.1086/316190
- Ferland, G.J., Porter, R.L., van Hoof, P.A.M., Williams, R.J.R., Abel, N.P., Lykins, M.L., Shaw, G., Henney, W.J., Stancil, P.C.: *RevMexA&Ap* **49**, 137 (2013). 1302.4485
- Frank, J., King, A., Raine, D.J.: *Accretion Power in Astrophysics: Third Edition*, Iii edition edn. Cambridge University Press, Cambridge (2002)
- Gaskell, C.M.: *ApJ* **263**, 79 (1982). doi:10.1086/160481
- Gaskell, C.M.: In: *Revista Mexicana de Astronomía y Astrofísica Conference Series. Revista Mexicana de Astronomía y Astrofísica*, vol. 27, no. 32, p. 1 (2008). 0711.2113
- Gaskell, C.M.: *New Astron. Rev.* **53**, 140 (2009). 0908.0386. doi:10.1016/j.newar.2009.09.006
- Gaskell, C.M., Goosmann, R.W.: *Astrophys. J.* **769**, 30 (2013). 0805.4258. doi:10.1088/0004-637X/769/1/30
- Goad, M.R., Korista, K.T.: *Mon. Not. R. Astron. Soc.* **444**, 43 (2014). 1407.5004. doi:10.1093/mnras/stu1456
- Hamann, F., Ferland, G.: *Astrophys. J.* **418**, 11 (1993). doi:10.1086/173366
- Hewett, P.C., Wild, V.: *Mon. Not. R. Astron. Soc.* **405**, 2302 (2010). 1003.3017. doi:10.1111/j.1365-2966.2010.16648.x
- Hu, C., Wang, J.-M., Ho, L.C., Chen, Y.-M., Bian, W.-H., Xue, S.-J.: *ApJL* **683**, 115 (2008). 0807.2060. doi:10.1086/591848
- King, A., Pounds, K.: ArXiv e-prints (2015). 1503.05206
- Kriss, G.: *Astronomical Data Analysis Software and Systems III*, A.S.P. Conference Series **61**, 437 (1994)
- Kuraszkiewicz, J., Wilkes, B.J., Schmidt, G., Smith, P.S., Cutri, R., Czerny, B.: *Astrophys. J.* **692**, 1180 (2009). doi:10.1088/0004-637X/692/2/1180
- Laor, A., Brandt, W.N.: *Astrophys. J.* **569**, 641 (2002). doi:10.1086/339476
- Loli Martínez-Aldama, M., Dultzin, D., Marziani, P., Sulentic, J.W., Bressan, A., Chen, Y., Stirpe, G.M.: *Astrophys. J. Suppl. Ser.* **217**, 3 (2015). 1501.04718. doi:10.1088/0067-0049/217/1/3
- Luo, B., Brandt, W.N., Hall, P.B., Wu, J., Anderson, S.F., Garmire, G.P., Gibson, R.R., Plotkin, R.M., Richards, G.T., Schneider, D.P., Shemmer, O., Shen, Y.: *Astrophys. J.* **805**, 122 (2015). 1503.02085. doi:10.1088/0004-637X/805/2/122
- Marziani, P., Sulentic, J.W.: *ApJ* **409**, 612 (1993). arXiv:astro-ph/9210005. doi:10.1086/172692
- Marziani, P., Sulentic, J.W.: *Mon. Not. R. Astron. Soc.* **442**, 1211 (2014). 1405.2727. doi:10.1093/mnras/stu951
- Marziani, P., Sulentic, J.W., Dultzin-Hacyan, D., Calvani, M., Moles, M.: *ApJS* **104**, 37 (1996). doi:10.1086/192291
- Marziani, P., Sulentic, J.W., Zwitter, T., Dultzin-Hacyan, D., Calvani, M.: *ApJ* **558**, 553 (2001). arXiv:astro-ph/0105343. doi:10.1086/322286
- Marziani, P., Sulentic, J.W., Zamanov, R., Calvani, M., Dultzin-Hacyan, D., Bachev, R., Zwitter, T.: *ApJS* **145**, 199 (2003a). doi:10.1086/346025
- Marziani, P., Zamanov, R.K., Sulentic, J.W., Calvani, M.: *MNRAS* **345**, 1133 (2003b). arXiv:astro-ph/0307367. doi:10.1046/j.1365-2966.2003.07033.x
- Marziani, P., Sulentic, J.W., Stirpe, G.M., Zamfir, S., Calvani, M.: *A&Ap* **495**, 83 (2009). 0812.0251. doi:10.1051/0004-6361:200810764
- Marziani, P., Sulentic, J.W., Negrete, C.A., Dultzin, D., Zamfir, S., Bachev, R.: *Mon. Not. R. Astron. Soc.* **409**, 1033 (2010). 1007.3187. doi:10.1111/j.1365-2966.2010.17357.x
- Marziani, P., Sulentic, J.W., Plauchu-Frayn, I., del Olmo, A.: *AAp* **555**, 89 (2013a). 1305.1096
- Marziani, P., Sulentic, J.W., Plauchu-Frayn, I., del Olmo, A.: *ApJ* **764**(150) (2013b). 1301.0520
- Marziani, P., Sulentic, J.W., Negrete, C.A., Dultzin, D., Del Olmo, A., Martínez Carballo, M.A., Zwitter, T., Bachev, R.: *Astrophys. Space Sci.* **356**, 339 (2015). 1410.3146. doi:10.1007/s10509-014-2136-z
- Nagao, T., Maiolino, R., Marconi, A., Matsuoka, K., Taniguchi, Y.: In: Peterson, B.M., Somerville, R.S., Storchi-Bergmann, T. (eds.) *IAU Symposium. IAU Symposium*, vol. 267, p. 73 (2010). doi:10.1017/S1743921-310005594

- Negrete, A., Dultzin, D., Marziani, P., Sulentic, J.: *ApJ* **757**, 62 (2012). 1107.3188
- Netzer, H., Brotherton, M.S., Wills, B.J., Han, M., Wills, D., Baldwin, J.A., Ferland, G.J., Browne, I.W.A.: *ApJ* **448**, 27 (1995). doi:10.1086/175939
- Netzer, H., Shemmer, O., Maiolino, R., Oliva, E., Croom, S., Corbett, E., di Fabrizio, L.: *Astrophys. J.* **614**, 558 (2004). arXiv:astro-ph/0406560. doi:10.1086/423608
- Osterbrock, D.E., Ferland, G.J.: *Astrophysics of Gaseous Nebulae and Active Galactic Nuclei*. University Science Books, Mill Valley, CA (2006)
- Peterson, B.M., Ferland, G.J.: *Nature* **324**, 345 (1986). doi:10.1038/324345a0
- Plotkin, R.M., Shemmer, O., Trakhtenbrot, B., Anderson, S.F., Brandt, W.N., Fan, X., Gallo, E., Lira, P., Luo, B., Richards, G.T., Schneider, D.P., Strauss, M.A., Wu, J.: *Astrophys. J.* **805**, 123 (2015). 1503.07523. doi:10.1088/0004-637X/805/2/123
- Punsly, B.: *Astrophys. J.* **713**, 232 (2010). 1002.4681. doi:10.1088/0004-637X/713/1/232
- Punsly, B., Zhang, S.: *Astrophys. J. Lett.* **735**, 3 (2011). 1105.1543. doi:10.1088/2041-8205/735/1/L3
- Reeves, J.N., O'Brien, P.T., Braitto, V., Behar, E., Miller, L., Turner, T.J., Fabian, A.C., Kaspi, S., Mushotzky, R., Ward, M.: *Astrophys. J.* **701**, 493 (2009). 0906.0312. doi:10.1088/0004-637X/701/1/493
- Richards, G.T.: In: Chartas, G., Hamann, F., Leighly, K.M. (eds.) *AGN Winds in Charleston*. Astronomical Society of the Pacific Conference Series, vol. 460, p. 67 (2012). 1201.2595
- Richards, G.T., Kruczek, N.E., Gallagher, S.C., Hall, P.B., Hewett, P.C., Leighly, K.M., Deo, R.P., Kratzer, R.M., Shen, Y.: *Astron. J.* **141**, 167 (2011). 1011.2282. doi:10.1088/0004-6256/141/5/167
- Rupke, D.S.N., Veilleux, S.: *Astrophys. J. Lett.* **729**, 27 (2011). 1102.4349. doi:10.1088/2041-8205/729/2/L27
- Shemmer, O., Trakhtenbrot, B., Anderson, S.F., Brandt, W.N., Diamond-Stanic, A.M., Fan, X., Lira, P., Netzer, H., Plotkin, R.M., Richards, G.T., Schneider, D.P., Strauss, M.A.: *Astrophys. J. Lett.* **722**, 152 (2010). 1009.2091. doi:10.1088/2041-8205/722/2/L152
- Snedden, S.A., Gaskell, C.M.: *ApJ* **669**, 126 (2007). doi:10.1086/521290
- Sulentic, J., Marziani, P., Zamfir, S.: *Baltic Astronomy* **20**, 427 (2011)
- Sulentic, J.W.: *Astrophys. J.* **343**, 54 (1989). doi:10.1086/-167684
- Sulentic, J.W., Marziani, P.: *ApJL* **518**, 9 (1999). arXiv:astro-ph/9904203. doi:10.1086/312060
- Sulentic, J.W., Marziani, P., Dultzin-Hacyan, D.: *ARA&A* **38**, 521 (2000). doi:10.1146/annurev.astro.38.1.521
- Sulentic, J.W., Marziani, P., Dultzin-Hacyan, D., Calvani, M., Moles, M.: *ApJL* **445**, 85 (1995). doi:10.1086/187896
- Sulentic, J.W., Marziani, P., Zwitter, T., Dultzin-Hacyan, D., Calvani, M.: *ApJL* **545**, 15 (2000). arXiv:astro-ph/0009326. doi:10.1086/317330
- Sulentic, J.W., Marziani, P., Zamanov, R., Bachev, R., Calvani, M., Dultzin-Hacyan, D.: *ApJL* **566**, 71 (2002). arXiv:astro-ph/0201362. doi:10.1086/339594
- Sulentic, J.W., Stirpe, G.M., Marziani, P., Zamanov, R., Calvani, M., Braitto, V.: *A&Ap* **423**, 121 (2004). arXiv:astro-ph/0405279. doi:10.1051/0004-6361:20035912
- Sulentic, J.W., Dultzin-Hacyan, D., Marziani, P., Bongardo, C., Braitto, V., Calvani, M., Zamanov, R.: *Revista Mexicana de Astronomia y Astrofisica* **42**, 23 (2006a). arXiv:astro-ph/0511230
- Sulentic, J.W., Repetto, P., Stirpe, G.M., Marziani, P., Dultzin-Hacyan, D., Calvani, M.: *A&Ap* **456**, 929 (2006b). arXiv:astro-ph/0606309. doi:10.1051/0004-6361:20054153
- Sulentic, J.W., Bachev, R., Marziani, P., Negrete, C.A., Dultzin, D.: *ApJ* **666**, 757 (2007). 0705.1895. doi:10.1086/519916
- Sulentic, J.W., Zamfir, S., Marziani, P., Dultzin, D.: In: *Revista Mexicana de Astronomia y Astrofisica Conference Series*. Revista Mexicana de Astronomia y Astrofisica Conference Series, vol. 32, p. 51 (2008)
- Sulentic, J.W., Marziani, P., del Olmo, A., Dultzin, D., Perea, J., Alenka Negrete, C.: *Astron. Astrophys.* **570**, 96 (2014). 1406.5920. doi:10.1051/0004-6361/201423975
- Tombesi, F., Sambruna, R.M., Reeves, J.N., Braitto, V., Ballo, L., Gofford, J., Cappi, M., Mushotzky, R.F.: *Astrophys. J.* **719**, 700 (2010). 1006.3536. doi:10.1088/0004-637X/719/1/700
- Trump, J.R., Hall, P.B., Reichard, T.A., Richards, G.T., Schneider, D.P., Vanden Berk, D.E., Knapp, G.R., Anderson, S.F., Fan, X., Brinkman, J., Kleinman, S.J., Nitta, A.: *Astrophys. J. Suppl. Ser.* **165**, 1 (2006). astro-ph/0603070. doi:10.1086/503834
- Tytler, D., Fan, X.-M.: *ApJS* **79**, 1 (1992). doi:10.1086/191642
- Véron-Cetty, M.-P., Véron, P.: *Astron. Astrophys.* **518**, 10 (2010). doi:10.1051/0004-6361/201014188
- Vestergaard, M.: *Astrophys. J.* **599**, 116 (2003). arXiv:astro-ph/0309550. doi:10.1086/379159
- Wisotzki, L., Christlieb, N., Bade, N., Beckmann, V., Köhler, T., Vanelle, C., Reimers, D.: *Astron. Astrophys.* **358**, 77 (2000). astro-ph/0004162
- Zamanov, R., Marziani, P., Sulentic, J.W., Calvani, M., Dultzin-Hacyan, D., Bachev, R.: *ApJL* **576**, 9 (2002). arXiv:astro-ph/0207387. doi:10.1086/342783
- Zamfir, S., Sulentic, J.W., Marziani, P.: *MNRAS* **387**, 856 (2008). 0804.0788. doi:10.1111/j.1365-2966.2008.13290.x
- Zamfir, S., Sulentic, J.W., Marziani, P., Dultzin, D.: *Mon. Not. R. Astron. Soc.* **403**, 1759 (2010). 0912.4306. doi:10.1111/j.1365-2966.2009.16236.x